IOP Conference Series: Materials Science and Engineering

PAPER • **OPEN ACCESS**

Bond characteristics of Al/Mg clad materials produced by vacuum roll bonding

To cite this article: J F Shu and T K Yamaguchi 2019 *IOP Conf. Ser.: Mater. Sci. Eng.* **576** 012031

View the article online for updates and enhancements.

This content was downloaded from IP address 59.127.168.43 on 15/10/2019 at 22:01

IOP Conf. Series: Materials Science and Engineering **576** (2019) 012031 doi:10.1088/1757-899X/576/1/012031

Bond characteristics of Al/Mg clad materials produced by vacuum roll bonding

J F Shu[1] and T K Yamaguchi[1]

[1]Department of Materials Science, Graduate School of Engineering, Kyushu Institute of Technology, Kitakyushu 804-8550, Japan

E-mail: yamaguchi.tomiko374@mail.kyutech.jp

Abstract. The A1050/AZ31 clad materials were produced by vacuum roll bonding. The effects of rolling temperature and reduction rate on the interface of A1050/AZ31 clad materials were investigated, and the fracture behaviors of A1050/AZ31 interface were studied. A very thin intermetallic compound layer was formed at the A1050/AZ31 interface at rolling temperature of 350 ℃ and reduction rate of 25%. Therefore the A1050/AZ31 interface mainly was ductile fracture, and the average tensile strength of A1050/AZ31 interface reached the maximum (43MPa). When the rolling temperature was 450 ℃ and the reduction rate was 25%, the fracture occurred on the brittle intermetallic compound Al_3Mg_2 layer (thickness 7.68μm) and $Al_{12}Mg_{17}$ layer (thickness 1.95μm), mainly on Al_3Mg_2 layer, and the average tensile strength of A1050/AZ31 interface reached the minimum (0.61MPa).

1. Introduction

Mg alloys as the lightest structural material and green engineering material are attracting much attention in the application of engineering [1, 2]. However, the applications of Mg alloys are still limited due to the poor corrosion resistant performance and weak deformability [3]. Therefore, it is particularly important to improve the disadvantage of Mg alloys.

In recent year, clad materials are being used in various fields since they exhibit excellent comprehensive performance [4-6]. Al is also a very light structural material, which is widely used in industry [7]. It can overcome demerits of Mg alloys by cladding an Al layer with corrosion resistance and good deformability on Mg alloy surfaces [8, 9]. At present, there are many processes can be used to produce Al/Mg clad materials. Roll bonding is an important technique to produce clad materials in industry [4, 10]. However, in the process of warm roll bonding, the oxide film is easy to produce and affect the performance of the interface [11]. The deterioration of oxide film can be effectively reduced under the vacuum condition. In this paper, Al/Mg clad materials were prepared by vacuum roll bonding.

2. Experimental

2.1. Materials and equipment

In this study, the pure industrial aluminium A1050 and Mg-Al-Zn alloy AZ31 plates were used. The dimensions of A1050 and AZ31 plates were 3mm×80mm×300mm, 1.5mm×65mm×200mm, respectively. The chemical compositions of A1050 and AZ31 are given in Table 1. A1050 and AZ31

Content from this work may be used under the terms of the Creative Commons Attribution 3.0 licence. Any further distribution of this work must maintain attribution to the author(s) and the title of the work, journal citation and DOI.
Published under licence by IOP Publishing Ltd

plates were annealed at 350 ℃ and 400 ℃ for 30min respectively. Before vacuum roll bonding, the AZ31 plate used #2000 sandpaper, and the A1050 plate used steel brush with the diameter of 3mm to remove the oxide films of the surface. The schematic diagram of the vacuum rolling equipment is shown in Figure 1. The materials were heated to rolling temperature through the high-frequency induction heating device and passed through the bonding roll. After rolling, the clad materials were cooled in vacuum.

Table 1. Chemical compositions of raw materials (mass %).

	Si	Cu	Mn	Zn	Ti	Fe	Mg	Al
A1050	0.25	0.05	0.05	0.05	0.03	0.4	0.05	Bal.
AZ31	0.07	0.05	0.27	0.69	-	0.003	Bal.	2.26

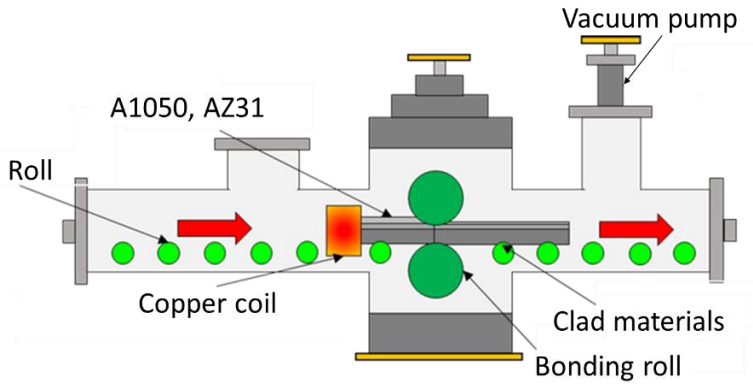

Figure 1. The schematic diagram of the vacuum rolling equipment.

2.2. Conditions

Keeping the vacuum degree (6mPa) and rolling speed (7mm/s) constant, the A1050/AZ31 clad materials were produced at various rolling temperature (350 ℃, 400 ℃, 450 ℃) and reduction rate (20%, 25%) by vacuum roll bonding. The reduction rates referred to in this paper are the total reduction rate of A1050/AZ31 clad materials. The bonding interfaces of the clad materials were observed and analyzed by scanning electron microscope (SEM) and electron probe X-ray microanalyzer (EPMA). To examine the interfacial properties, the tensile tests were performed at room temperature, and energy dispersive X-ray spectrometry (EDS) and X-ray diffraction (XRD) analyses were performed on the fracture surfaces.

3. Results and discussion

The reduction rate was an important parameter in the roll bonding process, affecting the bonding strength of the clad materials. Figure 2 shows the relationship between the reduction rate of A1050 and AZ31 and total reduction rate under different rolling temperatures. The abscissa is the total reduction rate of clad materials, and the longitudinal coordinate is the reduction rate of A1050 and AZ31. It can be seen from the graph that the reduction rates of A1050 are higher than the total reduction rate, and the reduction rates of AZ31 are lower than the total reduction rate. And the higher the rolling temperature at the same total reduction rate, the greater the difference between the reduction rate of A1050 and AZ31. This is because A1050 is FCC structure, and AZ31 is HCP structure. A1050 with more slip systems than AZ31 was easier to produce plastic deformation, and with the increase of rolling temperature plastic deformation capacity was greater.

3.1. Microstructures of the bonding interface

Figure 3 shows the interfacial microstructures of A1050/AZ31 clad materials at different rolling temperatures and reduction rates. It can be found from Figure 3(a) that no obvious diffusion layer was

observed at the A1050/AZ31 interface when the rolling temperature was 350 ℃. It can be seen from Figure 3(b)(c)(d) that a certain thickness of diffusion layers at the A1050/AZ31 interfaces were formed at rolling temperature of 400 ℃ and 450 ℃. And at the same temperature, the greater the reduction rate, the thicker the diffusion layer; at the same reduction rate, the higher the temperature, the thicker the diffusion layer. Therefore, when the rolling temperature was 450 ℃ and the reduction rate was 25%, the thickness of the diffusion layer was the largest.

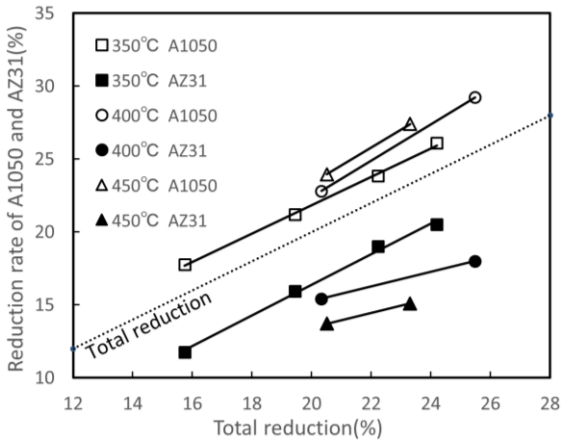

Figure 2. The relationship between the reduction rate of A1050 and AZ31 and total reduction rate under different rolling temperature.

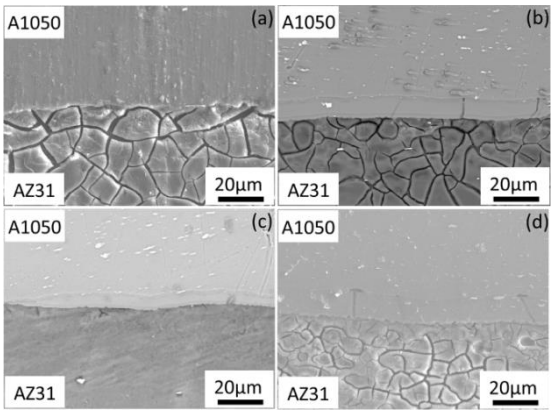

Figure 3. Interfacial microstructures of A1050/AZ31 clad materials at different rolling temperatures and reduction rates: (a) 350 ℃ 25%, (b) 400 ℃ 25%, (c) 400 ℃ 20%, (d) 450 ℃ 25%.

3.2. EPMA analysis

Figures 4 shows the results of EPMA area analysis of the A1050/AZ31 interface at rolling temperature of 350 ℃ and reduction rate of 25%. As seen in Figure 4, a very thin intermetallic compound layer was formed at the A1050/AZ31 interface. Figures 5 shows the results of EPMA area analysis of the A1050/AZ31 interface at rolling temperature of 450 ℃ and reduction rate of 25%. The results show that a certain thickness of the intermetallic compound layer was formed at the A1050/AZ31 interface. And the intermetallic compound of the A1050/AZ31 interface was formed on the A1050 side. This is because the diffusion activation energy of Mg atom in Al is much smaller than the diffusion activation energy of Al atom in Mg. Table 2 shows the results of EPMA point analysis of the diffusion layers. The atomic percentages of Mg in diffusion layer I and II were 40.57% and 58.23%, respectively. According to the Al-Mg alloy phase diagram, the chemical compositions in the diffusion layer I and II were intermetallic compounds Al_3Mg_2 (thickness 7.68μm) and $Al_{12}Mg_{17}$ (thickness 1.95μm), respectively.

3.3. Tensile strength of the bonding interface

The effects of rolling temperature and reduction rate on the tensile strength of A1050/AZ31 bonding interface are shown in Figure 6. From Figure 6, the tensile strength of A1050/AZ31 interface decreased with increasing rolling temperature. This was due to the formation of intermetallic compound of certain thickness during high temperature rolling, resulting in the decrease of tensile strength. In addition, when the rolling temperature was 350 ℃, the greater the reduction rate, the greater the tensile strength. However, low reduction rate got higher tensile strength at rolling temperature of 400 ℃ and 450 ℃. The main reason is that the higher reduction rate led to thicker intermetallic compound layer at high rolling temperature, as shown in Figure 3.

The average tensile strength of A1050/AZ31 interface reached maximum (43MPa) at rolling temperature of 350 ℃ and reduction rate of 25%. It was indicated that even though intermetallic compound was formed at the A1050/AZ31 interface, the thickness of the intermetallic compound layer

was too thin to play a leading role in the fracture. When the rolling temperature was 450 ℃ and the reduction rate was 25%, the average tensile strength of A1050/AZ31 interface reached minimum (0.61MPa). The main reason is that the thickness of intermetallic compound reached the maximum (Al_3Mg_2 7.68μm and $Al_{12}Mg_{17}$ 1.95μm) at this time. These intermetallic compounds are brittle and likely to deteriorate the bonding strength of A1050/AZ31 interface.

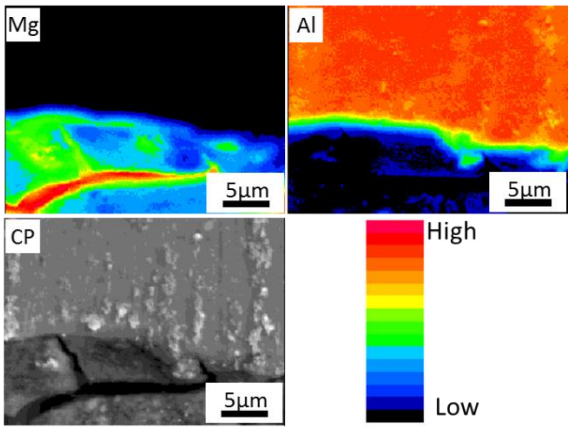

Figure 4. EPMA area analysis of A1050/AZ31 interface at rolling temperature of 350 ℃ and reduction rate of 25%.

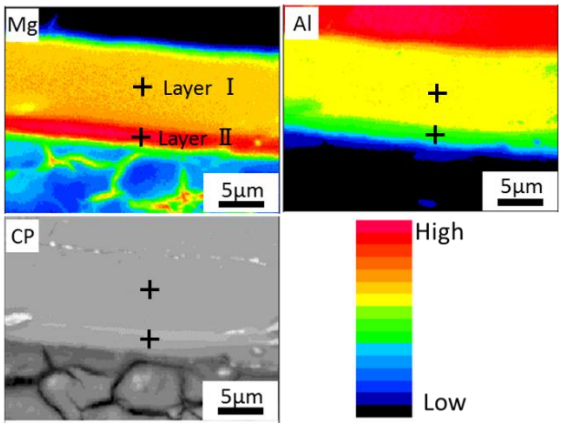

Figure 5. EPMA area analysis of A1050/AZ31 interface at rolling temperature of 450 ℃ and reduction rate of 25%.

Table 2. EPMA point analysis of the diffusion layers.

Diffusion layer	Mg/(Mg+Al) (at%)	Chemical composition
Ⅰ	40.57%	Al_3Mg_2
Ⅱ	58.23%	$Al_{12}Mg_{17}$

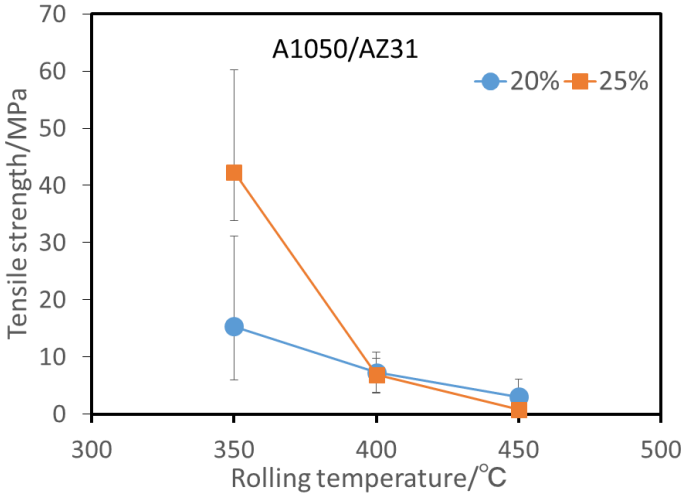

Figure 6. Effects of rolling temperature and reduction rate on the tensile strength of A1050/AZ31 interface.

3.4. Phase analysis of the fracture surface

The fracture surfaces of the tensile samples were analysed by XRD, and the results of A1050/AZ31 fracture surfaces are shown in Figure 7 and Figure 8. The results from figure 7 show that when the rolling temperature was 350 ℃ and the reduction rate was 25%, a small amount of the diffraction peaks of intermetallic compound Al_3Mg_2 were found on both sides of A1050 and AZ31, and Mg diffraction peaks were found on the A1050 side, while Al diffraction peaks were not detected on the AZ31 side. It is concluded that the fracture occurred mainly near the Mg side.

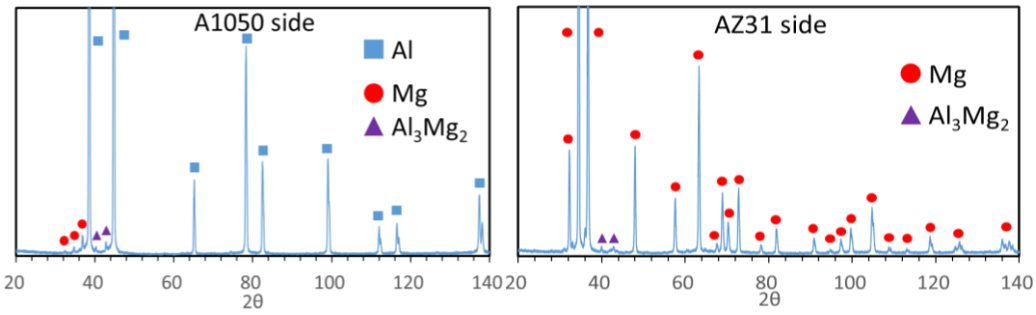

Figure 7. XRDPs of the A1050/AZ31 fracture surface at rolling temperature of 350 ℃ and reduction rate of 25%.

It can be seen from Figure 8 that in addition to the diffraction peaks of the main elements, the diffraction peaks of intermetallic compounds Al_3Mg_2 and $Al_{12}Mg_{17}$ appeared on both sides of A1050 and AZ31 at rolling temperature of 450 ℃ and reduction rate of 25%. Accordingly, combined with the analyses of EPMA, it is obvious that the fracture occurred mainly on intermetallic compound layers I (Al_3Mg_2) and II ($Al_{12}Mg_{17}$) in Figure 5. Furthermore, the amount of diffraction peaks of $Al_{12}Mg_{17}$ was very small. It can be further judged that most of the fracture occurred on layer I (Al_3Mg_2).

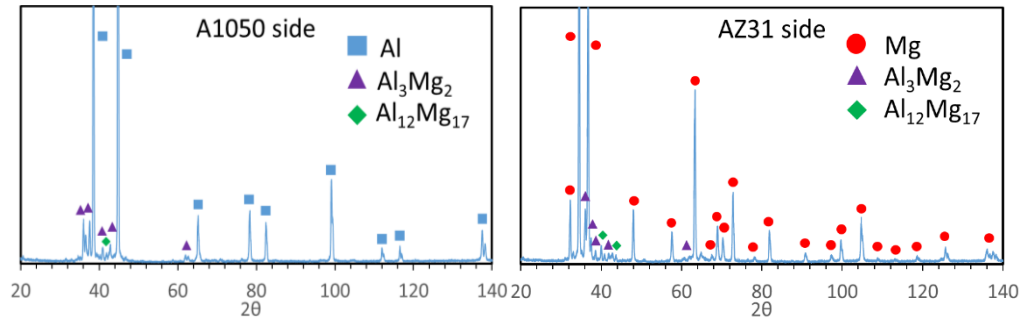

Figure 8. XRDPs of the A1050/AZ31 fracture surface at rolling temperature of 450 ℃ and reduction rate of 25%.

3.5. Morphology analysis of fracture surface

The fracture surfaces of the tensile samples were examined by SEM. Figure 9 shows the morphology of fracture surface of A1050/AZ31 interface at rolling temperature of 350 ℃ and reduction rate of 25%. According to Figure 9, the A1050/AZ31 interface mainly was ductile fracture, and there were a lot of dimples on the fracture surface of the AZ31 side. The brittle fracture also occurred simultaneously at the A1050/AZ31 interface, but it didn't play a leading role. This is because the intermetallic compound layer formed at the A1050/AZ31 interface was very thin.

Figure10 shows the morphology of fracture surface of A1050/AZ31 interface at rolling temperature of 450 ℃ and reduction rate of 25%. It can be seen that the A1050/AZ31 interface was brittle fracture. The EDS analysis of AZ31 side fracture surface is shown in Figure11. As can be seen from Figure 11, the distribution of Mg and Al elements on AZ31 side fracture surface was not very uniform, and the

content of Mg elements was obviously less. The content of Mg elements in area 1, 2, 3 was 38.05%, 58.01% and 63.38% respectively, as indicated in Table 3. Combined with the analyses of EPMA, The fracture of area 1 occurred on intermetallic compound layer I in Figure 5, and area 2, 3 occurred on intermetallic compound layer II in Figure 5. Furthermore, the fracture occurred mainly in the layer I (Al_3Mg_2). This result is the same as that of XRD.

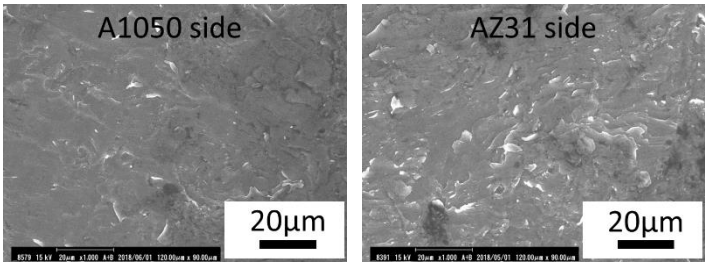

Figure 9. Morphology of fracture surface of A1050/AZ31 interface at rolling temperature of 350 ℃ and reduction rate of 25%.

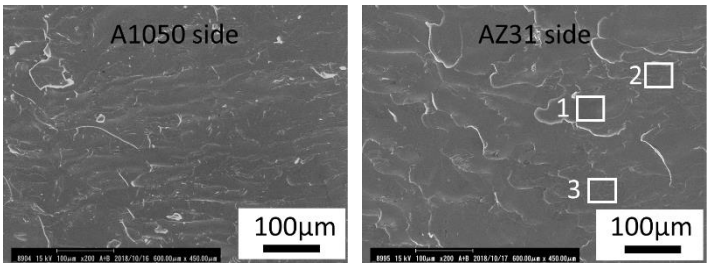

Figure 10. Morphology of fracture surface of A1050/AZ31 interface at rolling temperature of 450 ℃ and reduction rate of 25%.

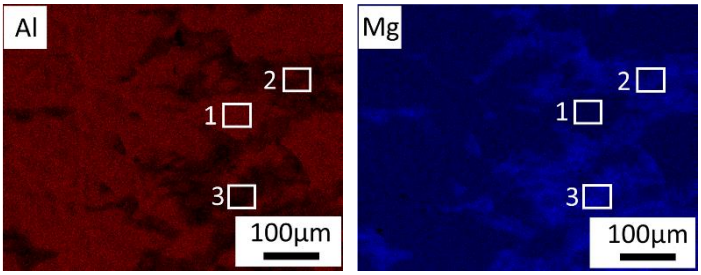

Figure 11. EDS analysis of AZ31 side fracture surface at rolling temperature of 450 ℃ and reduction rate of 25%.

Table 3. Element content in different regions of the AZ31 side.

Area	Mg(at%)	Al(at%)	Zn(at%)
1	38.05	60.87	0.8
2	58.01	41.02	0.66
3	63.38	35.29	1.04

4. Conclusions

In this paper, the A1050/AZ31 clad materials were produced by vacuum roll bonding, and bond characteristics of Al/Mg clad materials were studied. The conclusions are as follows:

(1) A very thin intermetallic compound layer was formed at the A1050/AZ31 interface at rolling temperature of 350℃. A certain thickness of intermetallic compound layers at the A1050/AZ31 interfaces were formed at rolling temperature of 400℃ and 450℃, and the greater the reduction rate, the greater the thickness.

(2) The tensile strength of A1050/AZ31 interface decreased with increasing rolling temperature. The average tensile strength of A1050/AZ31 interface reached the maximum (43MPa) at rolling temperature of 350℃ and reduction rate of 25%. Low reduction rate got higher tensile strength at rolling temperature of 400℃ and 450℃, so the average tensile strength of A1050/AZ31 interface reached minimum (0.61MPa) at rolling temperature of 450℃ and reduction rate of 25%.

(3) The influences of intermetallic compound on the fracture behaviors of A1050/AZ31 interface also were discussed. The intermetallic compound layer formed at the A1050/AZ31 interface was very thin at rolling temperature of 350℃ and reduction rate of 25%, therefore the A1050/AZ31 interface mainly was the ductile fracture. The intermetallic compound layers of Al_3Mg_2 (thickness 7.68μm) and $Al_{12}Mg_{17}$ (thickness 1.95μm) were formed in the diffusion zone at rolling temperature of 450℃ and reduction rate of 25%. Accordingly, the fracture occurred on Al_3Mg_2 layer and $Al_{12}Mg_{17}$ layer, and mainly on Al_3Mg_2 layer.

5. References

[1] Zhang J H, Liu S J, Wu R Z, Hou L G and Zhang M L 2018 *J. Magnes. Alloy* **6** 1-15
[2] Wei G B, Peng X D, Hu F P, Hadadzadeh A, Yang Y, Xie W D and Wells M A 2016 *Trans. Nonferrous Met. Soc. China* **26** 508-518
[3] Feng J W, Li H N, Deng K K, Fernandez C, Zhang Q R and Peng Q M 2018 *Corros. Sci.* **143** 229-239
[4] Zhang L, Meng L, Zhou S P and Yang F T 2004 *Mater. Sci. Eng. , A* **371** 65-71
[5] Yu H L, Lu C, Godbole A, Su L H, Sun Y, Liu M, Tang D L and Kong C 2013 *Sci. Rep.* **3** 1-9
[6] Nie H H, Liang W L, Chen H S, Zheng L W, Chi C Z and Li X R 2018 *Mater. Sci. Eng. , A* **732** 6-13
[7] Abbass M K, Hassan K S and Alwan A S 2015 *IJMMM* **3** 31-35
[8] Tokunaga T, Ohno M K and Matsuura K T 2018 *J. Mater. Sci. Technol.* **34** 1119-1126
[9] Mraied H, Cai W J and Sagüés A A 2016 *Thin Solid Films* **615** 391-401
[10] Wang Q, Leng X S, Yan J H, Guo W B, Fu Y and Luan T M 2013 *J. Mater. Csi. Technol.* **29** 948-954
[11] Xu Y, Hu L N and Sun Y 2013 *J. Alloy. Compd.* **580** 262-269